A four amino-acid linker between repeats in the α-synuclein sequence is crucial for fibril formation

Volodymyr V. Shvadchak and Vinod Subramaniam[*,†]

Nanobiophysics, MESA+ Institute for Nanotechnology& MIRA Institute for Biomedical Technology and Technical Medicine, University of Twente, Enschede, The Netherlands.

Supporting Information Placeholder

ABSTRACT: α-Synuclein is an 140 amino-acid protein that can switch conformation between intrinsically disordered in solution, helical on membrane, and β-sheet in amyloid fibrils. Using fluorescence of single tryptophan mutants we determined the immersion of different regions of the protein into lipid membranes. Our results suggest the presence of a flexible break at residues 52-55 between two helical domains. The 4 amino-acid linker is not necessary for membrane binding but is crucial for fibril formation. A deletion mutant lacking this linker aggregates extremely slowly and also slightly inhibits WT aggregation, possibly by blocking the growing ends of fibrils.

α-Synuclein (αSyn) is an 140 amino-acid intrinsically disordered protein highly expressed in the brain and localized at neural terminals.[1,2] Its physiological functions are yet unclear but are believed to be connected to the interaction with synaptic vesicles.[1,3,4] αSyn amyloid fibrils are the main component of Lewy bodies, intracellular inclusions in the brain of patients affected by Parkinson's Disease.[5]

αSyn consists of a hydrophobic region (residues 60-90) that serves as the amyloid fibril core,[3,6] an amphiphilic basic N-terminal part, and a negatively charged unstructured C-terminus. The protein sequence incorporates seven imperfect 11-residue xxKTKEGVxxx repeats (Fig. 1a).

αSyn shows remarkable conformational plasticity. It has no distinct secondary structure in solution but readily forms β-sheet rich amyloid fibrils upon aggregation and adopts α-helical structure upon membrane binding[7]. The presence of amphiphilic repeats in the N-terminal part inhibits fibrillization of αSyn[8] and determines membrane-binding affinity. αSyn binds anionic and rigid neutral membranes[9-11] and forms helices oriented parallel to the membrane surface[9,12,13] making 3 turns per 11 amino-acid repeat.[13] NMR of αSyn bound to SDS micelles shows two antiparallel α-helix fragments (residues 3-37 and 45-92).[12,14] The conformation of αSyn on lipid membranes was variously reported to be extended[13] or broken[15] α-helix depending on specific conditions.[9, 16] The position of the break is widely assumed to be the same as on micelles[14] but has not yet been conclusively experimentally demonstrated. The conformation of αSyn on membranes was studied by EPR[13] and fluorescence,[17-20] showing continuous periodic changes of the extent of immersion of residues 18 to 90 and the absence of membrane binding of the C-terminus.[10,12] Tryptophan fluorescence reports moderate immersion for the central part of αSyn but relatively deep insertion for N-terminal and NAC regions.[17, 21]

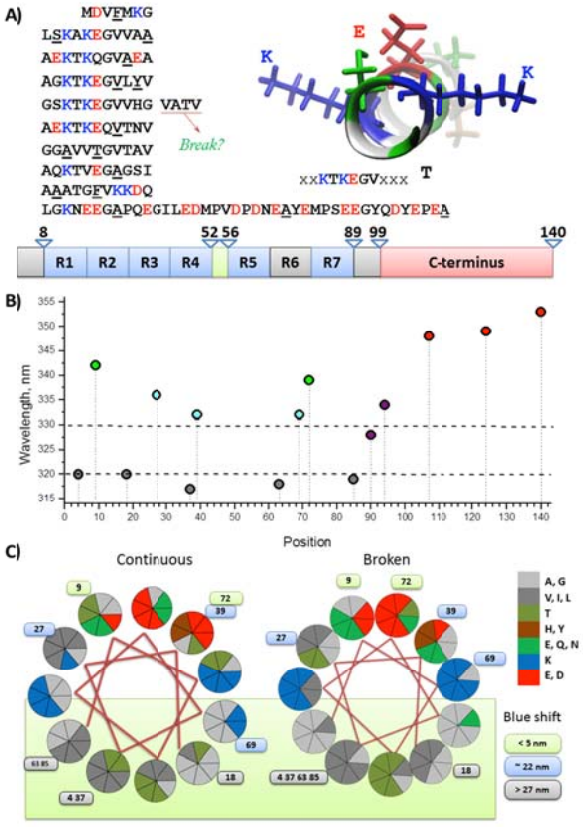

Fig 1. A) Amino-acid repeats in αSyn sequence. Residues mutated to Trp are underlined. Insert shows the structure of one 11 amino-acid repeat bound to SDS micelles.[14] B) Emission maxima of single Trp αSyn variants bound to DOPG vesicles. Size of symbols approximately corresponds to the experimental error (±1.5 nm). C) A wheel diagram of the αSyn repeat regions (residues 8-89) for continuous and broken helix models.

To analyze the conformation of membrane-bound αSyn we studied the immersion of 15 positions using fluorescence of single tryptophan mutants. In lipophilic environments the emission maxima of tryptophan fluorescence shift to the

blue, reflecting the extent of immersion into the membrane. All 15 mutants show similar affinity and final α-helix content with K_d ~ 0.25±0.1 μM and 40±10 lipid/protein stoichiometry upon binding to DOPG vesicles (Fig. S2), in agreement with previously published data (0.5 μM, 30±10 lipids/αSyn).[10] As expected, the changes of the Trp fluorescence emission upon membrane binding depend on the position. The strongest blue emission shifts (≥ 25 nm), corresponding to the deepest immersion, were observed for Trp at positions 4, 18, 37, 63, and 85, while positions 9 and 72 exhibit minor shifts, and labels on the flexible negatively-charged C-terminal tail show virtually no changes (Fig. 1b, Table S1). The observed differences in the membrane immersion of residues close in sequence, for example residues 4 and 9, is in good agreement with αSyn orientation parallel to the water-membrane interface and the correspondingly different environments for lipophilic and hydrophilic faces of the helix. The membrane immersion of amino-acids correlates to the position within the 11 amino-acid repeats (Fig. 1) in accordance with the 3/11 amino-acid periodicity of the protein helix.[13]

Two proposed models for membrane-bound αSyn are the extended, continuous[14] helix and the helix with a break.[15,16] In both cases the hydrophobic parts of the helices face the membrane, and the negatively-charged hydrophilic face and lysines are close to the membrane water interface (Fig. 1c). We studied 10 αSyn mutants containing Trp residues introduced in the repeat region (aa 8-89). For the continuous helix model (Fig. 1c, left) one would expect water-exposed residue 9; largely exposed residues 27, 39 and 72; and membrane immersion for the six other tested positions. In our experiments emission of tryptophan at positions 39 and 69 is similar and point to more apolar environment than of residues 9 and 72 but significantly less than that of residues 18, 63 or 85 (Fig. 1b, Table S1). These data better correlate to the model of a helix containing a break at the four amino-acid insert between the repeats (residues 52-55) (Fig. 1c, right). In this assumption the residues 4, 37, 63 and 85 are on the most immersed part of the helix (opposite to the acidic residues) while positions 39 and 69 are on the membrane-water interface. The broken helix conformation also shows more optimal distribution of lipophilic and hydrophilic residues on a wheel diagram (Fig. 1c), by removing membrane-immersed lysines and decreasing the number of water-exposed valines. The model with a break at amino-acids 38-44, similar to the structure on SDS micelles, would also fit the data but would require a difference in structure for very similar third and fourth 11 amino-acid repeats (Fig. S1).

We used mutants with Trp residues at positions 90, 94, 107, 124 and 140 to localize more precisely the end of the helical domain and the beginning of the C-terminal part of αSyn not involved in membrane binding. Tryptophan at positions 107, 124 and 140 shows no changes in fluorescence upon membrane binding, while αSyn-90W and -94W show significant blue shifts close to those observed for residues 39 and 69. Both continuous and broken helical conformations propose water-exposed positions for these two residues (Fig. S3) that do not match the observed blue-shifted emission. We suggest that αSyn adopts a helical conformation only in the repeat region and that residues 89-97 located after the last 11 amino-acid repeat are membrane-immersed but are not in the helical conformation due to the absence of proper periodicity in amino-acid polarity. This observation is in line with the average α-helix content calculated for αSyn based on CD spectroscopy (~60%) that corresponds to an ~84 aa long α-helix. The behavior of αSyn was very similar in charged (DOPG) and neutral (DPPC) membranes but significantly different in SDS micelles (Fig. S2). In SDS micelles, immersion of residues 37 and 39 was significantly lower than in lipid bilayers, perhaps reflecting increased solvent exposure in the break region reported in the NMR-based structure of SDS-bound αSyn.[14]

To validate our hypothesis of the break position (aa 52-55) of membrane bound αSyn we prepared a protein variant lacking these residues (αSynΔ). In the case of the continuous α-helix or another break position, such a construct should show significantly lower membrane affinity than WT αSyn due to the shift in the α-helix hydrophobicity pattern. Indeed, deletion of 4 residues (residues 2-5) at the N terminal alpha helix was reported to significantly decrease membrane binding.[22] Titration experiments show a moderate decrease in the binding affinity of αSynΔ compared to WT protein (Fig. S4). Moreover, tryptophan mutants αSynΔ-W37 and αSynΔ-W63 show emission spectra in the membrane-bound form almost identical to the αSyn-W37 and αSyn-W63 pointing to similar conformations on the membrane of protein regions flanking the repeat (Fig. S4). Taken together, these results allow us to conclude that the helix of membrane-bound αSyn contains a break close to residues 52-55.

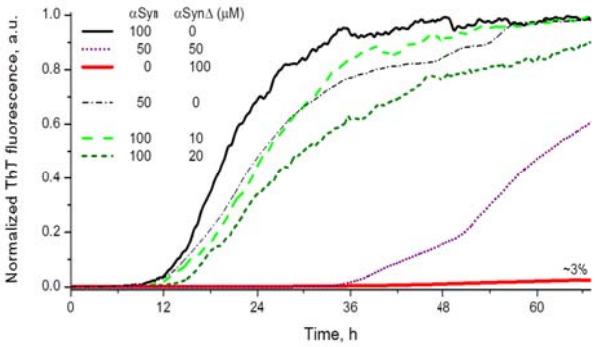

Figure 2. Aggregation of WT αSyn and αSynΔ monitored by ThT fluorescence. Averaged curves of 8 samples, normalized by maximal ThT fluorescence of 100 μM WT. 37°C, pH 7.2 phosphate buffer containing 150 mM NaCl.

A defining characteristic of αSyn is its ability to switch conformations between α-helix on membranes, random coil in solution and β-sheet in amyloid fibrils. Comparative analysis of mouse and human αSyn fibrils by solid state NMR suggests that residues 52-55 are in a beta-sheet region.[23] We tested the influence of the deletion of the 4 amino-acid linker on the protein aggregation propensity. The deletion mutant showed almost no tendency for aggregation compared to WT (Fig. 2). The aggregation of αSyn in the simplest model could be described as slow formation of oligomers that yield initial fibrils followed by relatively fast fibril growth.[24] Slower aggregation of αSynΔ compared to WT could be either because of less efficient initiation of fibril formation or due to slower fibril extension. To understand which of the two mechanisms predominates we checked if the WT αSyn could initiate aggregation of the deletion mutant in a mixture of 50 μM WT αSyn and 50 μM αSynΔ. Surprisingly, the aggregation rate of the mixture was significantly slower than that of the 50 μM WT αSyn alone, suggesting that not only

can WT αSyn not initiate aggregation of the deletion mutant but also that the mutant can inhibit aggregation of WT αSyn. The aggregation rate of WT also decreases upon addition of small amounts of αSynΔ; 10 and 20 mol.% αSynΔ slows down the aggregation by ~25% and ~40% respectively (Fig. 2). This could happen if the mutant binds the growing ends of fibrils and hinders their further extension. To check this hypothesis we estimated the relative content of αSynΔ in the fibril by aggregating mixtures where either WT αSyn or αSynΔ incorporated a Trp residue and by measuring the relative amounts in fibrils and solution by absorbance and fluorescence. The experiments show that aggregation of the mixture containing 50 μM WT and 50 μM αSynΔ leads to fibrils composed mostly of WT (>85%), leaving most of the deletion mutant in solution (Fig. S6). The low amount of αSynΔ in fibrils and its ability to decrease the aggregation rate of WT could possibly be explained by binding of αSynΔ to the fibrils ending with WT and subsequent inhibition of fibril growth due to the low affinity of both WT αSyn and αSynΔ to fibrils ending in the deletion mutant (Fig. S8).

Bousset et al. recently reported[25] on the formation of two distinct polymorphs of αSyn fibrillar structures at different salt concentrations, termed 'fibrils' and 'ribbons'. Residues 52-55 are incorporated into a beta sheet in 'fibrils' formed at physiological salt concentration but are suggested to be in a loop region in 'ribbons' formed at low salt conditions. We performed experiments at physiological salt concentrations. It is possible that αSynΔ could bind to fibril ends only in an alternative conformation corresponding to the low salt morphology that may decrease the affinity of the following αSyn monomer to be recruited to the fibril end, thus impairing fibril growth..

Our results suggest that the conformation of αSyn upon binding to membranes is determined by its 11 amino-acid repeat structure motif and consists of two 3/11 helical fragments (3-51) and (56-89), a short non-helical membrane immersed region (~89-95) and flexible soluble C-terminus. The break between the two helical parts corresponds to the 4 amino-acid linker in the sequence. A different position of the break could explain some of the discrepancies between results suggesting horseshoe and extended helix conformation of αSyn on membranes, since most reports assume that the position of the α-helix break is identical to that observed in SDS micelles.[12,14,26] The 11 amino-acid repeats motif and 4 amino-acid insertion after the fourth repeat is a common feature of α- , β- and γ-synucleins and play an important role in the conformational flexibility of the protein. The flexible insert between repeats is one of the key factors determining αSyn fibril growth.

ASSOCIATED CONTENT

Supporting Information

Materials, methods, supplementary figures and tables. This material is available free of charge via the Internet at http://pubs.acs.org.

AUTHOR INFORMATION

Corresponding Author

E-mail: subramaniam@amolf.nl; Phone: +31-20-7547100

Present Addresses

† FOM Institute AMOLF, Science Park 104, 1098 XG Amsterdam, The Netherlands.

Funding Sources

We acknowledge NanoNextNL project 3A.03 for support.

Notes

The authors declare no competing financial interests.

ACKNOWLEDGMENT

We thank Nathalie Schilderink and Kirsten van Leijenhorst-Groener for protein purification and Dr. Thomas M. Jovin (MPI-BPC, Göttingen) for access to the CD spectrometer.

REFERENCES

1. Bendor, J. T., Logan, T. P., and Edwards, R. H. (2013) *Neuron 79*, 1044-1066.
2. Iwai, A., Masliah, E., Yoshimoto, M., Ge, N., Flanagan, L., de Silva, H. A., Kittel, A., and Saitoh, T. (1995) *Neuron 14*, 467-475.
3. Lashuel, H. A., Overk, C. R., Oueslati, A., and Masliah, E. (2013) *Nat. Rev. Neurosci. 14*, 38-48.
4. DeWitt, D. C., and Rhoades, E. (2013) *Biochemistry 52*, 2385-2387.
5. Spillantini, M. G., Crowther, R. A., Jakes, R., Hasegawa, M., and Goedert, M. (1998) *Proc. Natl. Acad. Sci. U S A 95*, 6469-6473.
6. Chen, M., Margittai, M., Chen, J., and Langen, R. (2007) *J. Biol. Chem. 282*, 24970-24979.
7. Bisaglia, M., Mammi, S., and Bubacco, L. (2009) *FASEB J. 23*, 329-340.
8. Kessler, J. C., Rochet, J. C., and Lansbury, P. T., Jr. (2003) *Biochemistry 42*, 672-678.
9. Pfefferkorn, C. M., Jiang, Z., and Lee, J. C. (2012) *Biochim. Biophys. Acta 1818*, 162-171.
10. Shvadchak, V. V., Falomir-Lockhart, L. J., Yushchenko, D. A., and Jovin, T. M. (2011) *J. Biol.Chem. 286*, 13023-13032.
11. Nuscher, B., Kamp, F., Mehnert, T., Odoy, S., Haass, C., Kahle, P. J., and Beyer, K. (2004) *J. Biol. Chem. 279*, 21966-21975.
12. Chandra, S., Chen, X., Rizo, J., Jahn, R., and Sudhof, T. C. (2003) *J. Biol. Chem. 278*, 15313-15318.
13. Jao, C. C., Hegde, B. G., Chen, J., Haworth, I. S., and Langen, R. (2008) *Proc. Natl. Acad. Sci. U S A 105*, 19666-19671.
14. Ulmer, T. S., Bax, A., Cole, N. B., and Nussbaum, R. L. (2005) *J. Biol. Chem. 280*, 9595-9603.
15. Lokappa, S. B., and Ulmer, T. S. (2011) *J. Biol. Chem. 286*, 21450-21457.
16. Drescher, M., Huber, M., and Subramaniam, V. (2012) *ChemBioChem 13*, 761-768.
17. Pfefferkorn, C. M., and Lee, J. C. (2010) *J. Phys. Chem. B 114*, 4615-4622.
18. Mizuno, N., Varkey, J., Kegulian, N. C., Hegde, B. G., Cheng, N., Langen, R., and Steven, A. C. (2012) *J. Biol. Chem. 287*, 29301-29311.
19. Shvadchak, V. V., Yushchenko, D. A., Pievo, R., and Jovin, T. M. (2011) *FEBS Lett.585*, 3513-3519.
20. van Rooijen, B. D., van Leijenhorst-Groener, K. A., Claessens, M. M., and Subramaniam, V. (2009) *J. Mol. Biol. 394*, 826-833.
21. Wietek, J., Haralampiev, I., Amoussouvi, A., Herrmann, A., and Stöckl, M. (2013) *FEBS Lett. 587*, 2572-2577.
22. Vamvaca, K., Volles, M. J., and Lansbury, P. T., Jr. (2009) *J. Mol. Biol.* 389, 413-424.
23. Lv, G., Kumar, A., Giller, K., Orcellet, M. L., Riedel, D., Fernandez, C. O., Becker, S., and Lange, A. (2012) *J. Mol. Biol.* 420, 99-111.
24. Cohen, S. I., Vendruscolo, M., Welland, M. E., Dobson, C. M., Terentjev, E. M., and Knowles, T. P. (2011) *J. Chem. Phys. 135*, 065105.
25. Bousset, L., Pieri, L., Ruiz-Arlandis, G., Gath, J., Jensen, P. H., Habenstein, B., Madiona, K., Olieric, V., Bockmann, A., Meier, B. H., and Melki, R. (2013) *Nat. Commun. 4*, 2575.
26. Rao, J. N., Jao, C. C., Hegde, B. G., Langen, R., and Ulmer, T. S. (2010) *J. Am.Chem. Soc. 132*, 8657-8668.

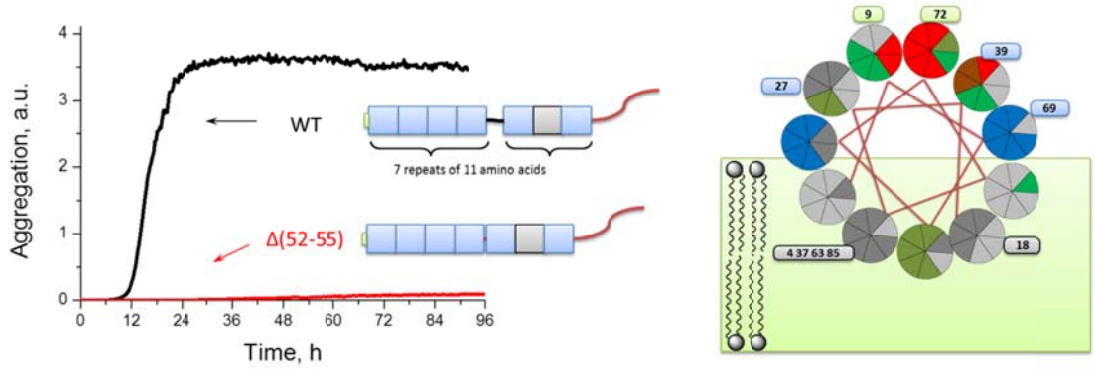

For Table of Contents Use Only

Supporting Information for

A four amino-acid linker between repeats in the α-synuclein sequence is crucial for fibril formation

Volodymyr V. Shvadchak and Vinod Subramaniam[*,†]

Nanobiophysics, MESA+ Institute for Nanotechnology& MIRA Institute for Biomedical Technology and Technical Medicine, University of Twente, Enschede, The Netherlands.

Materials and Methods

Vesicle preparation. Lipids in chloroform were purchased from Avanti Polar Lipids (Birmingham, USA). Stock solutions of 12.5 mM lipid were prepared in $CHCl_3$ and stored in glass vials at -20 °C. Aliquots of the appropriate amounts of the stock solutions were mixed in clean glass vials and the $CHCl_3$ was removed under a nitrogen stream and then rehydrated in 25 mM Na-PO_4, pH 7, 150 mM NaCl, to a final lipid concentration of 1 mM. Small unilamellar vesicles (SUVs) were prepared by sonication of the solution for 1 h at room temperature (DOPG) or 50±5°C (DPPC). The vesicles were used within 30h of preparation.

Synuclein expression and purification. The protein was prepared as described previously[20, 24]. Protein concentration was determined by measuring absorption at 280 nm, and using extinction coefficient values of ε=5300 for WT and αSynΔ, 9530 for Y39W and 10810 $cm^{-1}M^{-1}$ for other tryptophan mutants.

The deletion mutant lacking residues 52-55 (αSynΔ) was prepared using the same protocol as for WT.

Fluorescence emission spectra were recorded using a Fluoromax4 spectrofluorimeter (Horiba JobinYvon). For titration experiments 280 nm excitation wavelength and 5 nm slits were used. For fine maxima determination, emission spectra with excitation at 295 nm were also recorded to ensure the absence of tyrosine fluorescence. Spectra were corrected for vesicle scattering by blank subtraction and for wavelength dependence of detector sensitivity.

Binding constant determination. 1 or 2 μM solution of αSyn-Trp mutant was titrated by 1mM solutions of SUVs. The binding was monitored by fluorescence at 320 nm and 360 nm. The intensities were corrected for blank and for dilution of the solution. Titration curves (fluorescence intensity *vs* lipid concentration) were fitted to the single binding site model:

$$R = R_0 - (R_0 - R_F)\frac{K_d + P + L/n - \sqrt{(K_d + P + L/n)^2 - 4PL/n}}{2P} \qquad \text{(Eq.1)}$$

where the R_0 and R_F are initial and final signal respectively, P and L are the protein and lipid concentration and n is the number of lipids in one protein binding site. The binding stoichiometry was estimated both by extrapolating the linear part of the titration curve to the intersection with the final value and by direct fitting of the curves. For comparison of the membrane binding affinity of different αSyn mutants, the K_d were calculated assuming 30 lipids/protein binding stoichiometry.

Circular Dichroism Measurements. CD spectra were obtained with a Jasco J-720 spectropolarimeter. The protein concentration was 2μM. Spectra were recorded at room temperature (20°C) using a 2-mm path length cuvette. Scanning from 200 to 250 nm with a step size of 0.2 nm and a scanning speed of 20 nm/min, 6 averages, corrected for the background (protein-free vesicles). For the determination of $[\theta]_{222}$ the signal for 11 measurement points (221 to 223 nm) was averaged.

Aggregation. Aggregation experiments were performed in 96-well plates (200μL in each well) at 37°C and with shaking using a Tecan Infinite M200pro plate reader. Protein concentration was 100 μM. Buffer used was pH 7.2 Na-PO_4 6 mM, containing 150 mM NaCl, 9 mM NaN_3, 1 mM EDTA (to remove divalent ions bound to αSyn), and 5 μM ThT (5% of αSyn concentration). Aggregation was monitored by ThT fluorescence (excitation at 466 nm, emission at 485 nm), reading from the bottom of the plate.

Aggregation rate comparison. The solutions containing a) 50μM αSyn and 50 μM αSynΔ-W37 or b) 50μM αSyn-W37 and 50 μM αSynΔ was incubated at 37°C with shaking for 48h. Then they were 3-fold diluted with buffer and centrifuged (15000g, 15 min). Fibrils (with some residual solution) were separated from supernatant and both fractions were diluted to the same volume. The concentrations of αSyn and αSynΔ were estimated both by absorption at 295 nm and by the total Trp fluorescence intensity (excitation at 295 nm). Experiments were repeated in triplicates. The ratio of protein in supernatant and in fibrils was 0.65±0.3for WT and 9±4 for αSynΔ.

Table S1. Spectroscopic properties of αSyn tryptophan mutants.

Position	λ_{MAX} (DOPG), nm	Relative QY[a]	FWHM[b], nm	Expected[c] Continuous	Expected[c] broken	Observed[c]	Domain
4	321	0.94	47	++	++	++	
9	345	0.87	67	-	-	-	
18	321	0.40	60	++	++	++	
27	336	0.80	64	+/-	+/-	+/-	Helix 1
37	318	0.71	53	++	++	++	
39	332	0.45	66	+/-	+/-	+/-	
63	319	0.76	58	+	++	++	
69	333	0.48	63	+	+/-	+/-	
72	341	0.63	74	+/-	-	-	Helix 2
85	320	0.93	58	+	++	++	
90	328	0.23	71	-	-	+	Other
94	333	0.93	61	+/-	-	+/-	membrane immersed
107	345	0.93	66	--	--	--	Not
124	345	0.99	67	--	--	--	binding to
140	350	1	67	--	--	--	membrane

[a]Relative fluorescence quantum yield compared to αSyn-140W in buffer. [b]FWHM is the width of the emission band at half of intensity. [c]Expected and observed membrane immersion ranged from '--' (no changes) to '++' (deepest immersion).

```
      MDVFMKG
1  LSKAKEGVVAA
2  AEKTKQGVAEA
3  AGKTKEGVLYV
4  GSKTKEGVVHG VATV
5  AEKTKEQVTNV
6  GGAVVTGVTAV
7  AQKTVEGAGSI
   AAATGFVKKDQLGKNEEGAPQEGILEDMPVDPDNEAYEMPSEEGYQDYEPEA
```

Fig S1. Sequence of αSyn. The basic and acidic residues are colored blue and red respectively. The region between two helices on SDS micelles according to ref [14] is marked in yellow. The grey color is for the assumed nonhelical break region (residues 52-55). Residues are aligned according to the amino acids repeats (numbers on the left). Underlined amino acids show the Trp labeling positions used in this work. Double underlined residues were substituted for Trp also in the deletion mutant.

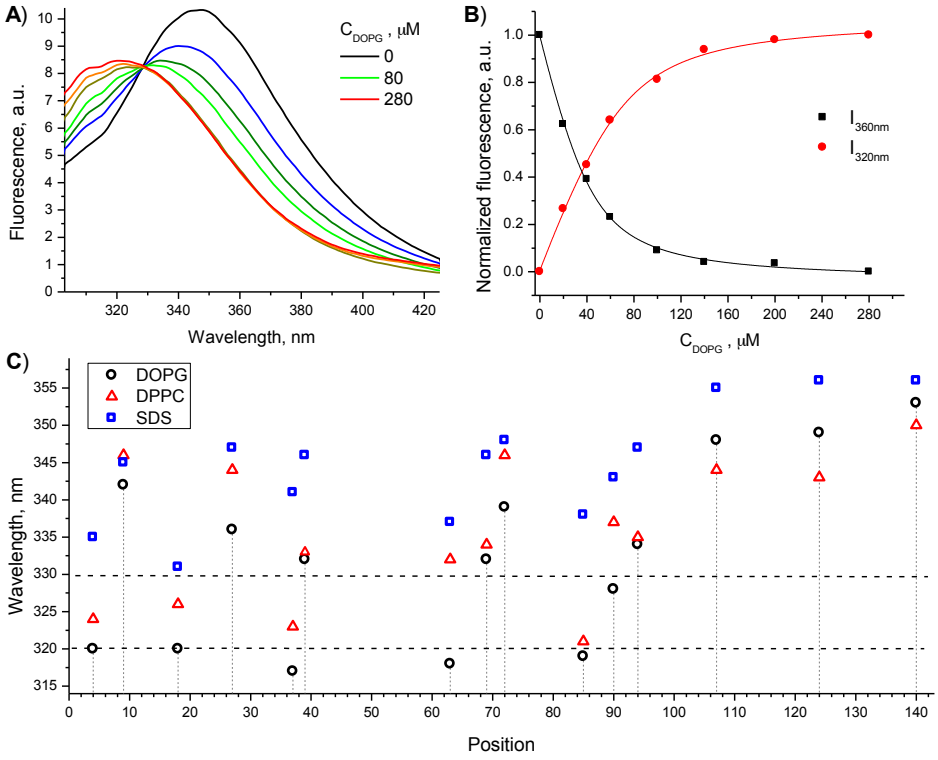

Figure S2. A) Fluorescence emission spectra of αSyn-W18 (2μM) at increasing DOPG concentrations. B) Normalized traces of fluorescence intensities at 360nm (black) and 320nm (red). Lines are fits of data to Eq1 giving K_d = 0.22±0.08μM and stoichiometry 33±5 lipids/protein. C) Tryptophan fluorescence emission maxima depending on the position on αSyn sequence in DOPG (circles), DPPC (triangles), and SDS (squares).

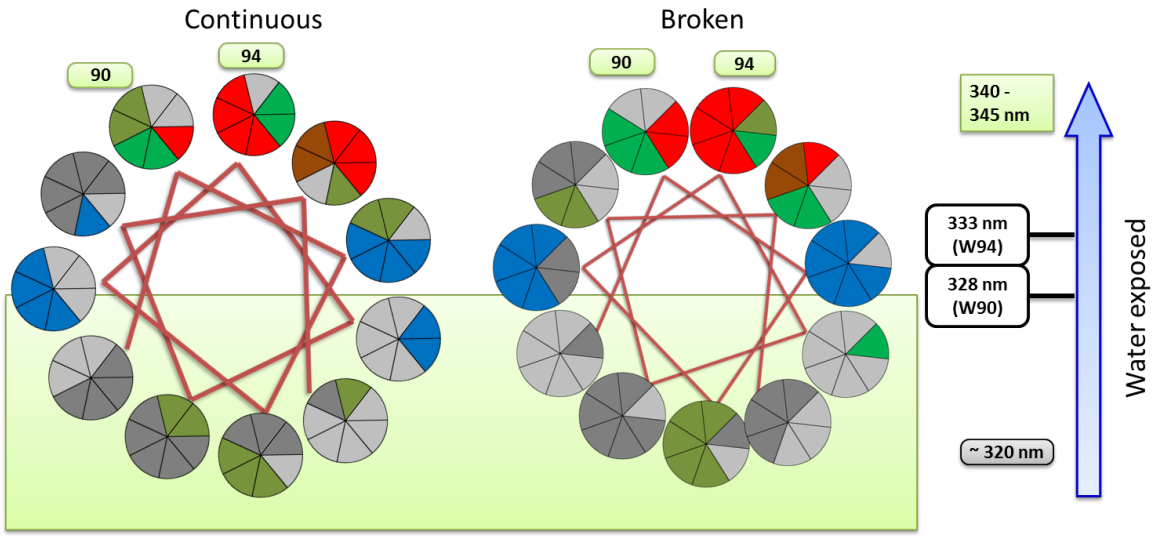

Figure S3. Expected positions of residues 90 and 94 assuming that they are in the helical part of the protein (green boxes). The Scale on the right shows typical positions for tryptophan emission at different immersion into membrane. 345 nm was observed for the most water exposed αSyn-W9 while immersed positions 4, 18, 37,63, 85 show values of 318-321 nm. White boxes show possible position of residues 90 and 94 relative to the water-membrane interface expected from the Trp emission maxima.

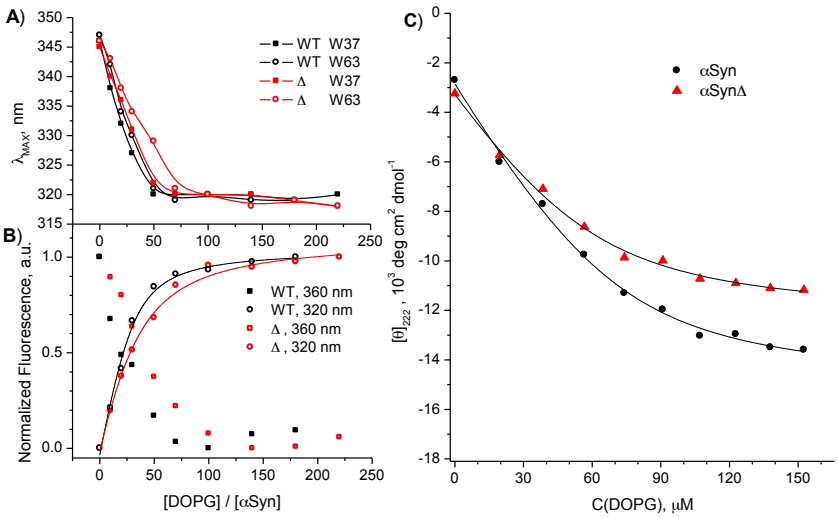

Figure S4. Comparison of the membrane binding affinity of αSyn and αSynΔ deletion mutant. A) Fluorescence emission maximum of Trp as function of DOPG concentration. B) Normalized fluorescence intensity of αSyn-63W and αSynΔ-63W. C) Mean residue ellipticity at 222 nm of αSyn (black), αSynΔ (red). For B) and C) lines are fits to Eq.1 assuming stoichiometry of 30 lipids per αSyn.

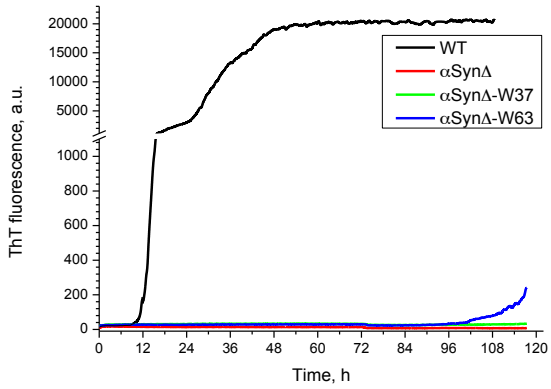

Figure S5. Comparison of aggregation rates of WT αSyn, αSynΔ, αSynΔ-W37, and αSynΔ-W63. Averages of 12 measurements (note the break of the scale).

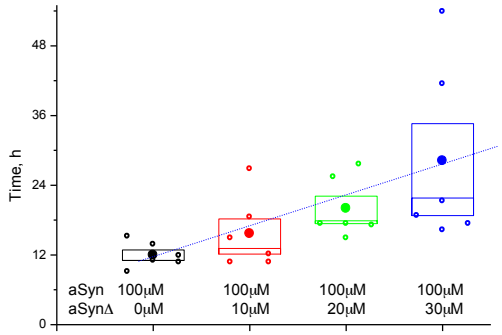

Figure S6. Inhibition of αSyn aggregation by αSynΔ measured at 100μM WT concentration. Results of 8 experiments. The fastest and the slowest traces were discarded. The graph shows the distribution of the time needed to reach 50% of the maximal intensity. Bold circles are the average values, boxes correspond to SD.